Supporting Information

Endothelial *microRNA-150* is an intrinsic suppressor of pathologic ocular neovascularization

Chi-Hsiu Liu[1], Ye Sun[1], Jie Li[1, 2], Yan Gong[1], Katherine T. Tian[1], Lucy P. Evans[1], Peyton C. Morss[1], Thomas W. Fredrick[1], Nicholas J. Saba[1], Jing Chen[1, *]

[1]Department of Ophthalmology, Boston Children's Hospital, Harvard Medical School, Boston, MA 02115, USA; [2]Department of Ophthalmology, Sichuan Provincial People's Hospital and Sichuan Academy of Medical Science, Chengdu, Sichuan 610027, China.

Short title: *MiR-150* suppresses ocular neovascularization

*To whom correspondence should be addressed. Email: jing.chen@childrens.harvard.edu

Supplementary information — Additional detailed methods

Bioinformatics

The conserved seed sequences of *miR-150* from different species, including human and murine, were obtained from miRBase (http://www.mirbase.org/) (1, 2). Potential targets of *miR-150* were predicted according to the algorithms of TargetScan (http://www.targetscan.org), MicroCosm (http://www.ebi.ac.uk/enright-srv/microcosm/htdocs/targets/v5/), and miRNA.org (http://www.microrna.org/microrna /home.do) with the parameters in default settings (3-6).

Laser-captured microdissection (LCM)

Eyes were enucleated from C57Bl/6J wild type mice at P17 exposed to either oxygen for OIR or room air for controls and embedded in optimal cutting temperature (OCT) compound (Tissue-Tek, Sakura Finetek USA, Inc., Torrance, CA, USA). 8 μm sections of each eye were isolated using a cryostat, mounted on ribonuclease (RNase)-free polyethylene naphthalate glass slides (Leica Microsystems; Wetzlar, Germany), followed by fixation in 70% ethanol followed by 90% and then 100% ethanol for 30 seconds in each solution before being washed with diethyl pyrocarbonate (DEPC)-treated water for 15 seconds. Sections were stained with isolectin B_4 (Invitrogen, Life Technologies, Grand Island, NY, USA) and treated with RNase inhibitor (Roche; Indianapolis, IN, USA) at 25 °C for 3 minutes. Retinal layers were then laser-capture microdissected with the Leica LMD 6000 system (Leica Microsystems) and collected directly into lysis buffer from the RNeasy Micro kit.

Laser-induced choroidal neovascularization (CNV)

Laser photocoagulation was carried out as described previously (7). 6-8 week-old *miR-150*$^{-/-}$ and WT mice were anesthetized and the pupils were dilated. Four laser burns were produced in the 3, 6, 9 and 12 o'clock positions around the optic disc with Micron IV retinal imaging system (Phoenix Research Lab, Pleasanton, CA, USA). At 1 week after laser treatment, CNV was analyzed in choroidal flat mounts with isolectin B_4 staining and lesion size was quantified. In addition, before killing mice fundus fluorescein angiography was performed to analyze fluorescein leakage. Briefly mice were anesthetized and injected intraperitoneally with Fluorescein AK-FLUOR® (100mg/ml, Akorn, Lake Forest, IL, USA) at 100μg/g (body weight). Fluorescent fundus images were taken with Micron IV at 5 and 10 minutes after injection. ImageJ was used by a masked observer to quantify the fluorescence intensity of CNV lesions with the lesion areas manually selected and measured using the "integrated intensity" function of ImageJ. The difference of integrated intensity between 5 and 10 minutes were recorded as an indicator of vascular leakage.

Retinal pigmented epithelial (RPE) cell isolation

RPE cells were isolated from 6-8 week-old adult mice. Mouse eyes were enucleated and the neural retinas were removed, revealing intact RPE attached to choroid/sclera. RPE cells were gently scraped from choroid/sclera complexes with a spatula under microscope, followed by RNA isolation for further analysis.

Cell culture

Human retinal microvascular endothelial cells (HRMECs) were obtained from Cell Systems Corporation (Kirkland, WA, USA), and cultured at 37°C with 5% CO_2 in a humid atmosphere using CSC complete medium (Cell Systems Corp). Human embryonic kidney 293T cells (HEK293T; ATCC, Manassas, VA, USA) were cultured in Dulbecco's modified Eagle's medium (DMEM; Invitrogen) supplemented with 10% fetal bovine serum (FBS; Invitrogen).

Transfection of *miR-150*

MiR-150 mimics and non-targeting scrambled negative control RNAs were used (Ambion, Life Technologies). Cells were transfected with 10 nM of *miR-150* mimics or negative control RNAs using siLentFect Lipid Reagent (Bio-Rad, Hercules, CA, USA) according to the manufacturer's instructions. Briefly, *miR-150* mimics or negative controls were complexed with the transfection reagent in serum free culture medium and added to HRMECs in fresh medium. Cells were then used for the following cell migration, MTT and tube formation assays after 24 hours transfection. FAM-labeled pre-miRNA (Ambion) was used as transfection indicator for analyzing transfection efficiency. Cells were transfected with 10 nM of FAM-labeled pre-miRNA using siLentFect Lipid Reagent for 24 hours, before being imaged for incorporation of fluorescence.

RNA isolation and cDNA preparation

Total RNA was extracted from the retinas and RPE cells of mice and from HRMECs. Retinas and cells were lysed with a homogenizing pestle and filtered through QiaShredder columns (Qiagen, Chatsworth, MD, USA). RNA was then extracted with an RNeasy Kit (Qiagen) according to the manufacturer's instructions. The RNA was then pooled to reduce biologic variability (for animal studies, n = 6; for non-animal studies, n = 3-5 per group). For cDNA preparation, 500 ng of total RNA was reverse transcribed using random hexamers, and SuperScript III Reverse Transcriptase (Invitrogen) according to the manufacturer's instructions. MiRNA was isolated from retinas of mice in OIR, normoxic and LCM (laser-captured microdissection) samples with the miRNeasy Micro Kit (Qiagen), and the cDNA was generated using the TaqMan miR reverse transcription kit (Applied Biosystems, Life Technologies) according to the manufacturers' instructions.

Quantitative polymerase chain reaction (qPCR)

Quantitative analysis of gene expression was determined using an ABI Prism 7700 Sequence Detection System (Applied BioSystems) and the SYBR Green Master Mix kit (Kapa Biosystems; Wilmington, MA, USA) with specific primers following manufacturer's instruction. Each target gene cDNA copy number was normalized to the house keeping gene, cyclophilin A (*CypA*) or β-actin (*ACTB*), using comparative CT (ΔΔCT) method. *MiR-150* expression level was also analyzed by qPCR with TaqMan miRNA Gene Expression Assays and TaqMan Universal PCR Master Mix (Applied Biosystems) according to the manufacturer's instructions. Data were quantified by ΔΔCT method and normalized to *U6* snRNA as the endogenous reference. A list of specific primers is available in **Table S1**.

Cell migration assay

HRMECs transfected with *miR-150* mimics or negative controls were seeded at a concentration of 2×10^5 cells/ml. After 24 hours of transfection, cells were treated with 10 μg/ml mitomycin C (Sigma-Aldrich, St. Louis, MO, USA) for 20 minutes at 37°C. Cell monolayers were wounded by scraping. For additional VEGF treatment, VEGF (20 ng/ml; R&D Systems, Minneapolis, MN, USA) in CSC serum-free medium supplemented with 1% FBS was added. Cells were then incubated at 37 °C for 14-18 hours. Images of cells were taken immediately after scraping and again after cell migration into wounded areas by a Zeiss AxioObserver.Z1 microscope (Oberkochen, Germany). For each image, the distance between the cells was measure, quantified and normalized to the original wound distance; three fields per well were counted (n = 4-5 per group) (8).

MTT assay

HRMECs were plated at a concentration of 2×10^5 cells/ml, transfected with *miR-150* mimics or negative controls, and incubated with DMEM at 37ºC for 24 hours. For additional VEGF treatment group, VEGF (20 ng/ml) in CSC serum-free medium supplemented with 1% FBS was added for 24 hours. Cell

proliferative activity was assayed using Vybrant MTT Cell Proliferation kit (Invitrogen) according to manufacturer's protocol. Absorbance was read at 570 nm by using xMark Microplate Spectrophotometer (Bio-Rad).

Tube formation assay

HRMECs transfected with *miR-150* mimics or negative controls were seeded in each well a 24-well plate, which were coated with Matrigel (BD Bioscience San Jose, CA, USA), at a density of 1×10^5 cells/well. For VEGF-treated group, medium containing 20 ng/ml of VEGF was added. Cells were incubated at 37°C for 6 hours and then imaged by Zeiss AxioObserver.Z1 microscope to assess the formation of tube-like structures. The total tube length, number of junctions, number of meshes and percentage of mesh area were analyzed by the Angiogenesis Analyzer plug-in for ImageJ (9) (n = 3-6 per group).

Luciferase reporter assay

The oligonucleotides comprising the *miR-150* target sequences were synthesized by Invitrogen, and annealed and cloned into pmirGLO vectors (Promega, Madison, WI, USA) for luciferase reporter assays. The *miR-150* target sequences within the 3′ untranslated regions (UTRs) of each target gene were predicted by TargetScan, MicroCosm, and miRNA.org as described previously (3-6). Constructs containing sequences with the *miR-150* seed-matched sites (**Table S2**) were confirmed by sequencing at the Boston Children's Hospital IDDRC Molecular Genetics Core Facility. HEK293T cells were plated into 96-well plates at 2×10^4 cells/well and transfected with the reporter plasmids containing target sequences or empty vectors as controls using Lipofectamine 2000 (Invitorgen). Cells were co-transfected with 10 and 50 nM *miR-150* mimics or negative controls. After 24 hours, luciferase activity was measured using the Dual-Glo Luciferase Assay System (Promega). Firefly luciferase activity was normalized to *Renilla* luciferase activity and to negative controls.

Aortic ring assay

Aortic ring assays were performed as described previously (10). 4-week old *miR-150*$^{-/-}$ and WT mice were euthanized (n=3 per group). Aortae were dissected, cut into 1-mm-thick rings, embedded in 30 µl of growth factor-reduced Matrigel (BD Biosciences) in 24-well tissue culture plates containing CSC complete medium (Cell Systems Corp), and incubated at 37ºC with 5% CO_2 for 8 days. For explants treated with VEGF, 20 ng/ml of VEGF in serum-free medium with 1% FBS was added on the third day. Medium was changed every 48 hours for all groups. Images of individual explants were taken from 4 days after plating using a ZEISS AxioOberver.Z1 microscope. The vascular sprouting area was quantified with a semi-automated macro plug-in for ImageJ.

Choroid sprouting assay

Choroidal sprouting experiments were performed as previously described (11). The RPE/choroid from 4-week old *miR-150*$^{-/-}$ and WT mouse were cut into approximately 1×1 mm^2 pieces (n=3 per group), and placed in growth factor-reduced Matrigel (BD Biosciences) in 24-well plates with CSC complete medium (Cell Systems Corp). Choroidal explants were incubated at 37ºC for 7 days with growth medium being changed every other day. For explants treated with VEGF, 20 ng/ml of VEGF in serum-free medium with 1% FBS was added on the third day. Images of individual explants were taken from 3 days after embedding and the area of microvascular sprouting was quantified using SWIFT_Choroid method, which is a macro plug-in for ImageJ.

Analysis of *rd8* Mutation

PCR-based analysis of *rd8* mutation was performed as described previously (12). Briefly, genomic DNA was isolated from mouse tails using DNAzol® (Invitrogen) according to the manufacturer's instructions. The WT allele and *rd8* mutant allele were detected using specific primers described by Mattapallil et al. [mouse crumbs homolog 1 (m*Crb1*) forward-1: 5'-GTGAAGACAGCTACAG TTCTGATC-3'; m*Crb1* forward-2: 5'-GCCCCTGTTTGCATGGAGGAAACTTGGAAGACAGCTA CAGTTCTTCTG-3'; and m*Crb1* reverse: 5'-GCCCCATTTGCACACTGATGAC-3']. All 3 specific primers, which result in 2 sets of primers, were used in each reaction to genotype the mice. The predicated size of *rd8* mutant band is 244 bp, and the WT band is 220 bp. For further confirmation, PCR products were purified using a QIAquick PCR Purification Kit (Qiagen) and sequenced at the Boston Children's Hospital Molecular Genetics Core Facility.

Supplementary information — References:

1. Griffiths-Jones S, Grocock RJ, van Dongen S, Bateman A, & Enright AJ (2006) miRBase: microRNA sequences, targets and gene nomenclature. *Nucleic acids research* 34(Database issue):D140-144.
2. Kozomara A & Griffiths-Jones S (2014) miRBase: annotating high confidence microRNAs using deep sequencing data. *Nucleic acids research* 42(Database issue):D68-73.
3. Betel D, Koppal A, Agius P, Sander C, & Leslie C (2010) Comprehensive modeling of microRNA targets predicts functional non-conserved and non-canonical sites. *Genome biology* 11(8):R90.
4. Betel D, Wilson M, Gabow A, Marks DS, & Sander C (2008) The microRNA.org resource: targets and expression. *Nucleic acids research* 36(Database issue):D149-153.
5. Grimson A*, et al.* (2007) MicroRNA targeting specificity in mammals: determinants beyond seed pairing. *Molecular cell* 27(1):91-105.
6. Lewis BP, Shih IH, Jones-Rhoades MW, Bartel DP, & Burge CB (2003) Prediction of mammalian microRNA targets. *Cell* 115(7):787-798.
7. Li J*, et al.* (2014) Endothelial TWIST1 Promotes Pathological Ocular Angiogenesis. *Investigative ophthalmology & visual science* 55(12):8267-8277.
8. Gong Y*, et al.* (2013) Sprouty4 regulates endothelial cell migration via modulating integrin beta3 stability through c-Src. *Angiogenesis* 16(4):861-875.
9. Carpentier G, Martinelli M, Courty J, & Cascone I (2012) Angiogenesis Analyzer for ImageJ. *4th ImageJ User and Developer Conference proceedings*, pp 198-201.

10. Baker M*, et al.* (2012) Use of the mouse aortic ring assay to study angiogenesis. *Nature protocols* 7(1):89-104.
11. Shao Z*, et al.* (2013) Choroid sprouting assay: an ex vivo model of microvascular angiogenesis. *PloS one* 8(7):e69552.
12. Mattapallil MJ*, et al.* (2012) The Rd8 mutation of the Crb1 gene is present in vendor lines of C57BL/6N mice and embryonic stem cells, and confounds ocular induced mutant phenotypes. *Investigative ophthalmology & visual science* 53(6):2921-2927.

Number of Supplemental Tables: 2

Number of Supplemental Figures: 9

Supplementary information — Tables

Table S1. Primers for qPCR

Gene	Forward (5'→3')	Reverse (5'→3')
Mouse		
Cdh5	ATTGGCCTGTGTTTTCGCAC	CACAGTGGGGTCATCTGCAT
Cxcr4	GACTGGCATAGTCGGCAATG	AGAAGGGGAGTGTGATGACAAA
CypA	CAGACGCCACTGTCGCTTT	TGTCTTTGGAACTTTGTCTGCAA
Dll4	TTCCAGGCAACCTTCTCCGA	ACTGCCGCTATTCTTGTCCC
Fzd4	TTCCTTTGTTCGGTTTATGTGCC	CTCTCAGGACTGGTTCACAGC
Vegfa	AGAGGCTTGGGGCAGCCGAG	ACTCCCGGGCTGGTGAGTCC
Vegfr1	GTCACAGATGTGCCGAATGG	TGAGCGTGATCAGCTCCAGG
Vegfr2	CAAACCTCAATGTGTCTCTTTGC	AGAGTAAAGCCTATCTCGCTGT
Human		
CXCR4	GACTGGCATAGTCGGCAATG	AGAAGGGGAGTGTGATGACAAA
DLL4	GCGAGAAGAAAGTGGACAGG	ACAGTAGGTGCCCGTGAATC
FGF2	AGTGTGTGCTAACCGTTACCT	ACTGCCCAGTTCGTTTCAGTG
FZD4	GCCAATGTGCACAGAGAAGA	GGCAAACCCAAATTCTCTCA
LRP5	CTTCCACACTCGCTGTGAGG	GGCAGGCGCATGTGTAGAA
LRP6	TGCAAACAGACGGGACTTGAG	CGGGGACAATAATCCAGAAACAA
NOTCH1	CCCTTGCTCTGCCTAACGC	GGAGTCCTGGCATCGTTGG
VEGFA	AGGGCAGAATCATCACGAAGT	AGGGTCTCGATTGGATGGCA
VEGFR1	GAAAACGCATAATCTGGGACAGT	GCGTGGTGTGCTTATTTGGA
VEGFR2	AGCGGGGCATGTACTGACGATTAT	AGCGGGGCATGTACTGACGATTAT
ACTB	AGAGCTACGAGCTGCCTGAC	AGCACTGTGTTGGCGTACAG

Table S2. Oligonucleotide sequences for luciferase reporter constructs

Gene	Seed Position	Sequences (5'→3')*
CXCR4	1819-1825	AATGCTGGTTTTTCAGTTTTCAGGAGTGGGTTGATTTCAGCACCT
DLL4	2504-2510	CATATGCAACGTGCTGCTCTCAGGAGGAGGAGGGAATGGCAGGAA
FZD4	4156-4162	CACGCTCTGCTCTGGTGTCTTGGGAGTTGTGCAGGGACTCTGGCC

*****The *miR-150* seed sequence-matched sites are underlined.

Supplementary information — Figures and Figure legends

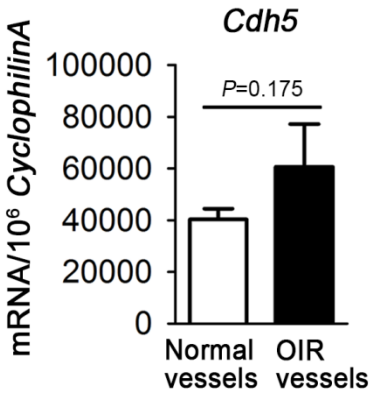

Figure S1. Comparable expression levels of *Cdh5* in LCM-isolated pathologic retinal vessels versus normal vessels. Expression levels of *Cdh*5, encoding endothelial cell marker VE-cadherin, showed no significant difference between normal retinal vessels from normoxic retinas and pathological vascular tufts isolated from OIR retinas at P17 (n = 6 per group). Expression levels were normalized to cyclophilin A (*CypA*). Data were presented as mean ± SEM.

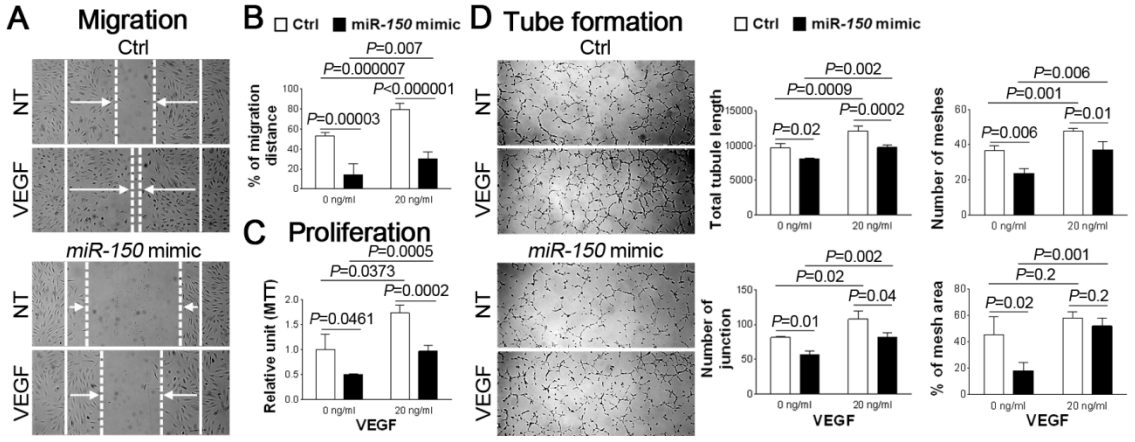

Figure S2. Effects of *miR-150* on HRMEC proliferation, migration and tube formation in the presence of VEGF. (**A**) Representative images of HRMEC migration assay treated with *miR-150* mimic combined with VEGF. The solid lines present the starting position of cell migration, the dash lines indicate the end position of cell migration, and the arrows indicate the direction of migration. (**B**) Quantitative analysis of HRMEC migration showed that cells treated with *miR-150* mimic revealed suppressed migration abilities in both VEGF and non-treated (NT) group, compared to respective negative mimic control (Ctrl) transfected groups (n = 4-5 per group). (**C**) MTT assay results showed that *miR-150* transfected HRMECs had lower levels of proliferation activities in both VEGF treatment and non-treated groups, compared to control mimic-treated groups (n = 3 per condition). (**D**) Representative images and quantitative analysis of tube formation assay characterizing tubule length, junction numbers, mesh numbers, and the percentage of mesh area. HRMECs transfected with *miR-150* mimic showed decreased capacity of tubular formation compared to negative mimic control, in both VEGF-treated and non-treated groups (n = 3-5 per group). NT: non-treated (0 ng/ml of VEGF); VEGF: 20 ng/ml. Data were presented as mean ± SD.

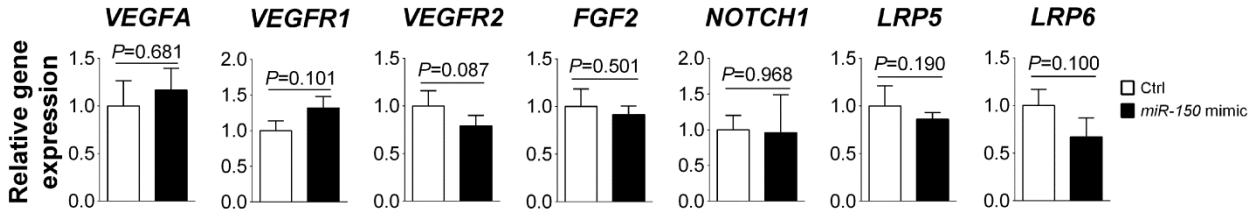

Figure S3. *MiR-150* did not affect gene expression levels of *VEGFA*, *FGF2*, *VEGFR1, VEGFR2, NOTCH1, LRP5* and *LRP6* in HRMECs. Expression levels of *VEGFA, VEGFR1, VEGFR2, FGF2, NOTCH1, LRP5* and *LRP6* were not substantially altered in HRMECs treated with *miR-150* mimic compared with negative control mimic (Ctrl) (n = 3 per condition). Results were normalized to *ACTB* and to expression levels in mimic control. Data were presented as mean ± SD.

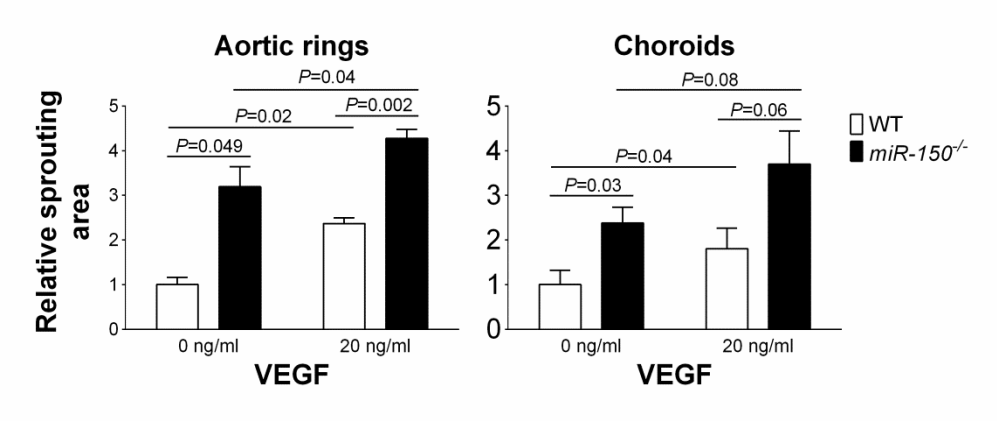

Figure S4. Effects of *miR-150* deficiency on aortic ring and choroidal explant vascular sprouting in the presence of VEGF. Aortic rings and choroids explants isolated from 4 week-old WT and *miR-150*$^{-/-}$ mice showed increased sprouting ability in presence of VEGF *ex vivo* (n = 3 per group). Deficiency of *miR-150* results in exacerbated relative sprouting areas compared to WT, when co-treated with VEGF. Data were presented as mean ± SEM.

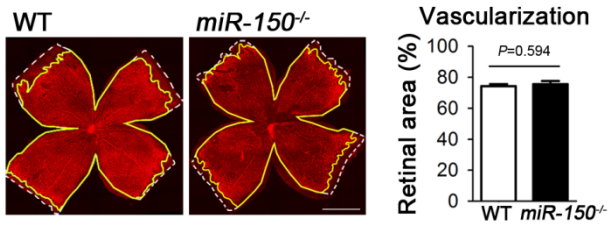

Figure S5. Similar levels of physiological retinal vascular growth in WT and *miR-150*$^{-/-}$ mice. Retinal flat mounts from P7 WT and *miR-150*$^{-/-}$ mice were stained with isolectin B_4 (red) to visualize blood vessels. Both groups of mice showed normal retinal vasculature with comparable levels of vascularized retinal areas (yellow lines) expressed as percentage of total retinal areas (white dash lines) (n = 4 or 5 per group). Data were presented as mean ± SEM. Scale bar represents 1 mm.

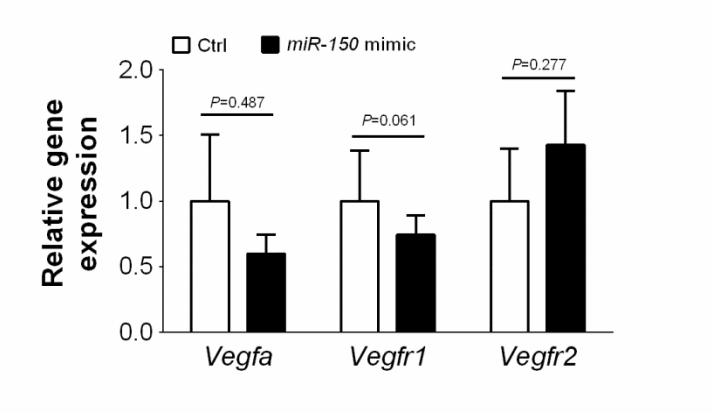

Figure S6. Expression levels of *Vegfa, Vegfr1 and Vegfr2 in* OIR retinas treated with *miR-150*. In P17 WT OIR retinas with injection of *miR-150* mimic or negative mimic control (Ctrl), expressing levels of *Vegfa*, *Vegfr1* and *Vegfr2* revealed no significant difference. Expression levels were normalized to *CypA* and relative to contralateral eyes injected with mimic control (n = 3 per group). Data were presented as mean ± SEM.

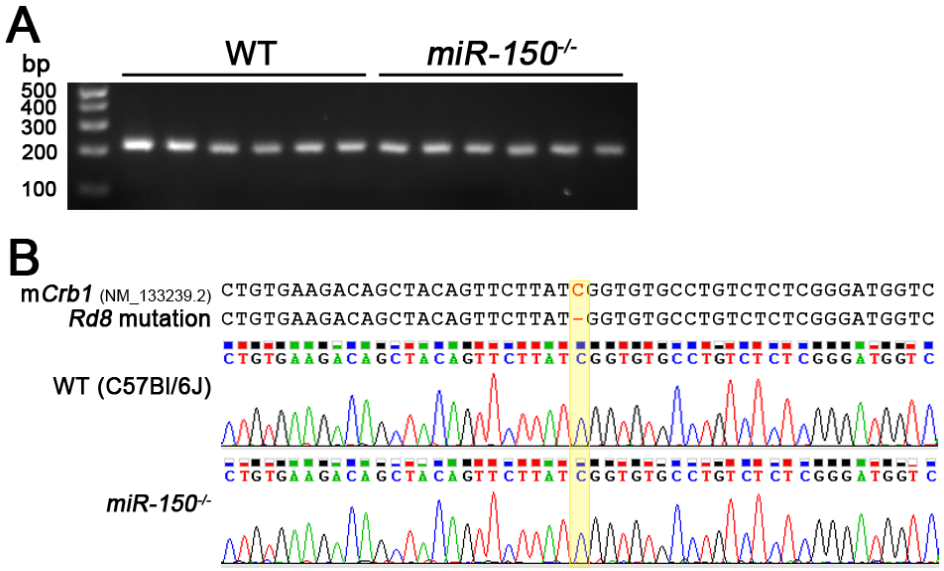

Figure S7. Genetic analysis confirming the absence of *rd8* (*Crb1*) mutation in WT and *miR-150*$^{-/-}$ mice. (**A**) Gel electrophoresis image of PCR products derived from WT and *miR-150*$^{-/-}$ mouse tails (n = 6 per group) amplified with *rd8* detection primers. The wild type allele PCR product is 220 bp, and the *rd8* allele PCR product is 244 bp. PCR products from *miR-150*$^{-/-}$ tails showed single band (~220 bp) of comparable size as WT (C57Bl/6J) mice, which were known to contain no *rd8* mutation as described by Mattapallil et al. (*IOVS*, 2012). (**B**) Sequencing of mouse *Crb1* gene (m*Crb1*) in both WT and *miR-150*$^{-/-}$ mice showed no single base deletion of *rd8* mutation at the expected position (yellow shade), confirming the absence of *rd8* mutation in both WT and *miR-150*$^{-/-}$ mouse stains.

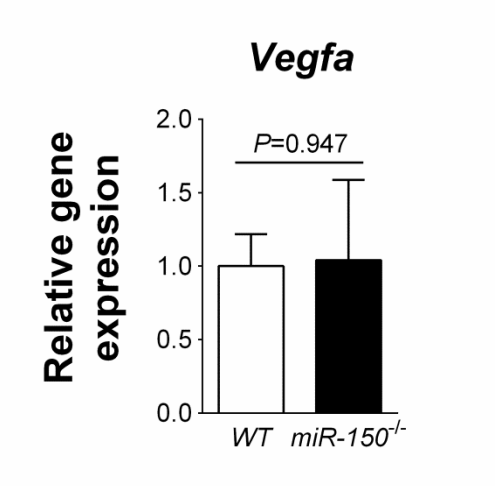

Figure S8. Expression levels of *Vegfa in* RPE isolated from WT and *miR-150*$^{-/-}$ mice. *Vegfa* expressing levels were comparable in RPE isolated from 6-8week-old WT and *miR-150*$^{-/-}$ mouse eyes (n = 4 per group). Expression levels were normalized to *CypA* and to WT groups. Data were presented as mean ± SEM.

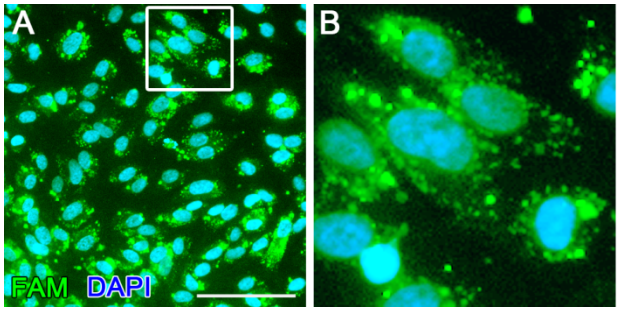

Figure S9. Transfection of FAM-labeled pre-miRNA as an indicator of miRNA transfection efficiency. (**A**) Representative image of HRMECs transfected with FAM-labeled pre-miRNA (green) counterstained with DAPI (blue) for analyzing transfection efficiency. 24 hour after transfection, random images were taken from each well of a 6-well plate. Based on the quantification of fluorescent uptake in ~3000 cells analyzed, transfection efficiency was 90.8±4.2%. (**B**) A higher magnification image of the FAM-positive cells with successful transfection of FAM-labeled pre-miRNA. Scale bar presents 100 μm.